IL NUOVO CIMENTO Vol. 35 C, N. 6 Novembre-Dicembre 2012
DOI 10.1393/ncc/i2012-11375-5

Colloquia: LaThuile12

Electroweak physics at the Tevatron

V. Cavaliere on behalf of the CDF and DØ Collaborations
University of Illinois - Urbana - Champaign, IL, USA

ricevuto il 7 Settembre 2012

Summary. — We present a review of the recent Tevatron diboson measurements in leptonic and semileptonic decay modes. The most stringent limits on anomalous triple gauge couplings are reported for each final state.

PACS `14.70.Fm` – W bosons.
PACS `14.70.Hp` – Z bosons.
PACS `13.38.Be` – Decays of W bosons.
PACS `13.38.Dg` – Decays of Z bosons.

1. – Introduction

Following the ending of the Tevatron collider program, we can review the significant progress that has been made in the diboson sector over the ten years of Run 2. The availability of theoretical tools such as MCFM [1] and MC@NLO [2] has allowed the standard model to be tested in the diboson sector. Measuring diboson production is a fundamental as it is an important electroweak process and a major background to Higgs searches. Furthermore, measuring diboson production allows access to triple gauge couplings, which could provide indications of new physics.

2. – $W\gamma$ and $Z\gamma$

The most up to date measurement of $W\gamma$ and $Z\gamma$ production comes from the DØ Collaboration that analyzed $4.2\,\mathrm{fb}^{-1}$ and $6.2\,\mathrm{fb}^{-1}$ of data, respectively [3].

The event selection for $W\gamma$ starts by requiring an electron or muon, a photon, and missing transverse energy. The analysis uses a neural network for photon identification to improve sensitivity to $WW\gamma$ coupling. Backgrounds are at the 20–25% level, overwhelmingly W+jets, and are estimated from data. An important property of the standard model prediction at leading order is that interference between the s- and t-channel amplitudes produces a zero in the total $W\gamma$ yield at a specific angle $\theta*$ between the W boson and the incoming quark in the $W\gamma$ rest frame. Although it is difficult to measure the angle directly, this so-called radiation amplitude zero is also visible in the charge-signed

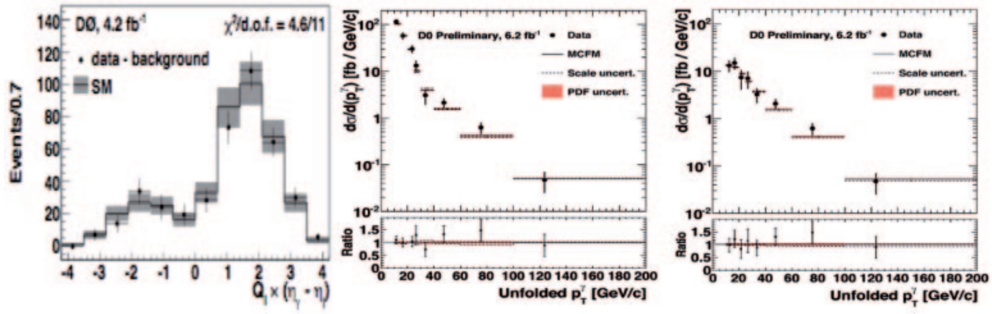

Fig. 1. – Left: charge-signed photon-lepton rapidity difference. The radiation zero amplitude can be seen as a dip at $-1/3$. Center and right: the differential cross-section $\mathrm{d}\sigma/\mathrm{d}p_T(\gamma)$ for all $M(\ell\ell\gamma)$, and for the ISR-dominated sample $M(\ell\ell\gamma) > 110\,\mathrm{GeV}/c^2$.

photon-lepton rapidity difference as a dip at around $-1/3$. Figure 1 shows the dip, compared with the signal prediction. The measured cross-section for the kinematic region $E_T(\gamma) > 15\,\mathrm{GeV}$ and $\Delta R(\ell\gamma) >$ is $7.6 \pm 0.4(\mathrm{stat}) \pm 0.6(\mathrm{sys})\,\mathrm{pb}$, in good agreement with the standard model prediction of $7.6 \pm 0.2\,\mathrm{pb}$. If there were anomalous triple gauge couplings, the photon E_T spectrum would be modified and more high-E_T photons observed. The photon E_T spectrum may therefore be used to derive limits on anomalous $WW\gamma$ couplings. A binned likelihood fit to data is used, and the 1-d limits 95% CL limits obtained are $-0.4 < \Delta\kappa\gamma < 0.4$ and $-0.08 < \lambda_\gamma < 0.07$ for a new physics scale $\Lambda = 2\,\mathrm{TeV}$.

Also the $Z\gamma$ analysis uses a neural network technique to provide a robust differentiation between photons and jets. Background is at the 5 10% level and is dominated by Z+jets. The $Z\gamma$ system has the property that initial state photon radiation (ISR) may be selected preferentially over final state photon radiation by requiring the three-body invariant mass $M(\ell\ell\gamma)$ to be above the Z boson mass. With $M(\ell\ell\gamma) > 110\,\mathrm{GeV}/c^2$, around 300 events are observed in each of the final states. The differential cross-section $\mathrm{d}\sigma/\mathrm{d}p_T(\gamma)$ is measured, using matrix inversion to unfold the experimental distribution, and is shown in fig. 1 both for all $M(\ell\ell\gamma)$, and for the ISR-dominated sample $M(\ell\ell\gamma) > 110\,\mathrm{GeV}/c^2$. The data are compared with the NLO prediction from MCFM, and are seen to be consistent. Total cross-sections are also quoted: for the kinematic region $|\eta(\gamma)| < 1$, $E_T(\gamma) > 10\,\mathrm{GeV}$, $\Delta R(\ell\gamma) > 0.7$ and $M(\ell\ell\gamma) > 60\,\mathrm{GeV}/c^2$ the result is $1.09 \pm 0.04(\mathrm{stat}) \pm 0.07(\mathrm{sys})\,\mathrm{pb}$, to be compared with the standard model prediction of $1.10 \pm 0.03\,\mathrm{pb}$; and for $M(\ell\ell\gamma) > 110\,\mathrm{GeV}/c^2$ the result is $0.29 \pm 0.02(\mathrm{stat}) \pm 0.01(\mathrm{sys})\,\mathrm{pb}$, to be compared with the standard model prediction $0.29 \pm 0.01\,\mathrm{pb}$.

3. – Heavy diboson production

3˙1. *Leptonic decay channels: WZ and ZZ.* – These final states are characterized by low branching ratio and clean yields. All the analysis use improved lepton definitions to increase the acceptance.

The WZ production in $\ell\ell\ell\nu$ final state had been studies by CDF using $7.1\,\mathrm{fb}^{-1}$ of integrated luminosity [4]. The analysis incorporates improvements in lepton selection and uses a neural network to separate the signal from the background (ZZ contribution is the biggest). The measured cross-section is found to be $\sigma(p\bar{p} \to WZ) = (3.9^{+0.6}_{0.5}(\mathrm{stat})^{+0.6}_{0.4}(\mathrm{syst}))\,\mathrm{pb}$ in good agreement with the SM prediction of $3.46 \pm 0.21\,\mathrm{pb}$.

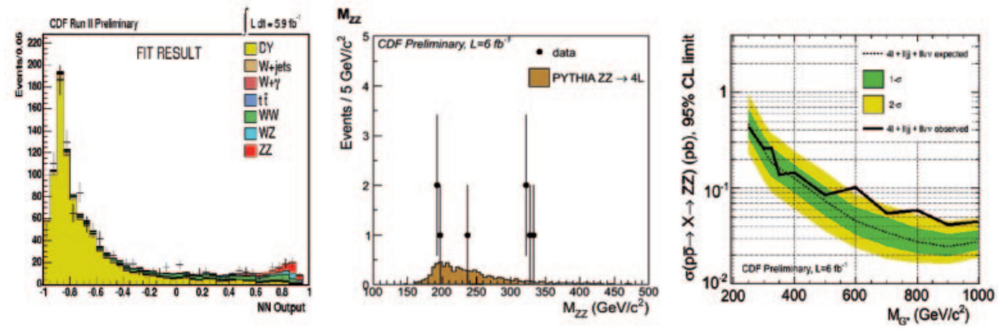

Fig. 2. – Left: NN output for ZZ to four lepton analysis. Center: M_{ZZ} distribution shows the clustering of events around $325\,\mathrm{GeV}/c^2$. Right: Limits on the presence of a Randall-Sundrum (RS) graviton decaying to two Z bosons.

Triple gauge couplings limits are extracted from the Zp_T distribution for a new physics scale of 1.5 and 2.0 TeV. The DØ Collaboration has also performed an measurement of the WZ cross-section in this final state and of ZZ production in four leptons [5]. The peculiarity of these analyses is that they do not restrict the offline event selection to events satisfying specific trigger conditions but analyse all recorded data in order to maximise the event yields. For the WZ cross-section a likelihood fit to the M_T is performed, while for the ZZ a neural network output is used as a discriminator. The systematic uncertainties are reduced by taking the ratio to the measured $Z \to \ell\ell$ cross-section and then multiplying for the theoretical calculation of the Z boson production cross-section. The results are $\sigma(p\bar{p} \to WZ) = 4.50 \pm 0.61(\mathrm{stat.})^{+0.16}_{-0.25}(\mathrm{syst.})$ pb and $\sigma(p\bar{p} \to ZZ) = 1.64 \pm 0.44(\mathrm{stat.})^{+0.13}_{-0.15}(\mathrm{syst.})$ pb, in agreement with the SM prediction.

CDF has also new measurement of the ZZ production cross-section in the four-lepton final state and $\ell\ell\nu\nu$ using $6\,\mathrm{fb}^{-1}$ of integrated luminosity [6]. The four lepton analysis uses a counting experiment, while for $ZZ \to \ell\ell\nu\nu$ that is afflicted by a large Drell-Yan background contribution a NN is used to extract the cross-section (see fig. 2a). The combination of the two analysis leads to $\sigma(p\bar{p} \to ZZ) = 1.64^{+0.44}_{-0.38}$ pb. These final states together with the semileptonic ones are used to search for ZZ resonances [7]. A clustering of events at high mass is observed (see fig. 2). However, analysis of the other ZZ final states $ZZ \to \ell\ell\nu\nu$ and $ZZ \to \ell\ell jj$ showed them to be more sensitive to a resonance of mass around $325\,\mathrm{GeV}/c^2$ decaying to ZZ, and the data in those channels are in agreement with standard model predictions (limits are set using a Randall-Sundrum (RS) graviton decaying to two Z bosons see fig. 2). The four-lepton events therefore appear to arise from standard model sources.

3·2. *Semileptonic decay channels.* – Given their similarity to key Higgs boson signatures, there have been ongoing efforts to observe diboson production in final states with jets.

Two CDF analyses observed WW and WZ production in the $\ell\nu jj$ final state in 2010. This final state is very similar to that expected from WH associated production. W+jets is the overwhelming background. In the first analysis the signal was extracted from a χ^2 fit to the dijet mass distribution as shown in fig. 3, giving an extracted cross-section $\sigma(WW + WZ) = (18.1 \pm 3.3(\mathrm{stat}) \pm 2.5(\mathrm{sys}))$ pb with 5.2σ significance [8]. The second analysis used a matrix element technique, for which the final event probability

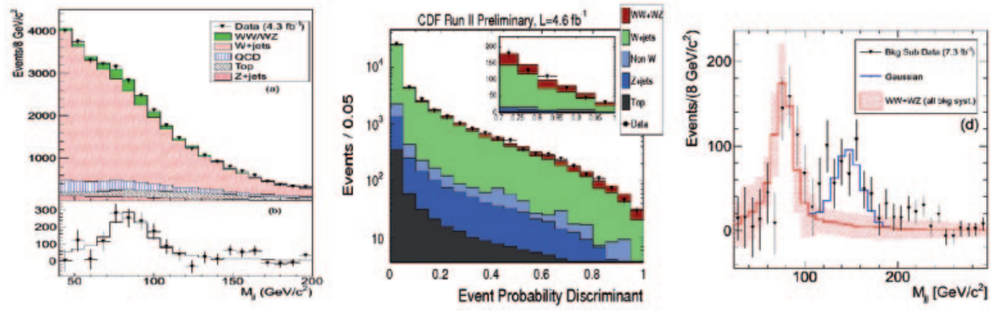

Fig. 3. – Left: Dijet mass spectrum in WW/WZ analysis showing the diboson contribution. Center: Matrix Element Discriminator for WW/WZ analysis. Right: Dijet mass spectrum for W+2jet event with harder cuts showing the excess around $150\,\mathrm{GeV}/c^2$.

discriminant is shown in fig. 3. Here, the extracted cross-section was $\sigma(WW+WZ) = (16.5^{+3.3}_{-3.0})\,\mathrm{pb}$, with 5.4σ significance [8]. The first analysis was also used to look for higher mass resonances. A 4.1σ excess is observed in dijet mass spectrum of W+2jet sample [9], as shown in fig. 3c. Studies are still in progress to understand the cause of the excess. The DØ Collaboration tried to replicate the analysis and found no significant discrepancy with the respect to the background model.

DØ also updated their measurement in the $\ell\nu jj$ final state, using $4.3\,\mathrm{fb}^{-1}$ of integrated luminosity [10]. A random forest multivariate discriminant is used to separate signal from background, and since Z bosons can decay to b-quark pairs but W bosons cannot, b-tagging is employed both to improve the significance of the observation, and to separate the WW and WZ components. Both the random forest discriminant output, and the dijet invariant mass for the no b-tag data sample, are shown in fig. 4. A cross-section $\sigma(WW+WZ) = 19.6^{+3.1}_{-3.0}\,\mathrm{pb}$ is measured, with 8σ significance, and contours of the separated WW and WZ cross-sections are given in fig. 4.

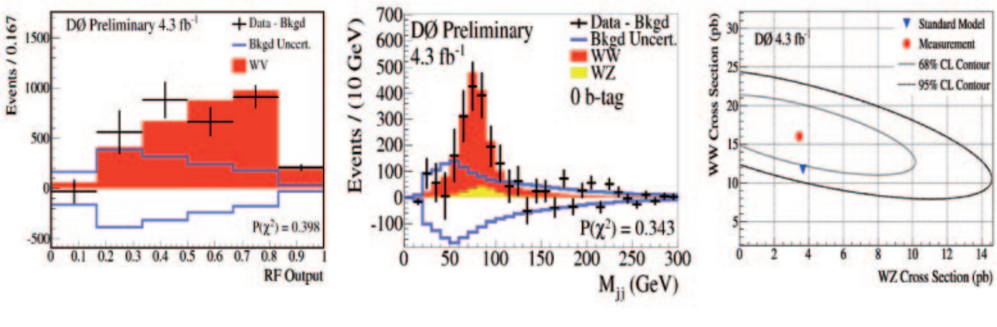

Fig. 4. – Results from DØs WW/WZ analysis in the $\ell\nu jj$ final state: (left) random forest multivariate discriminant output; (centre) background-subtracted dijet mass; (right) contours of WW and WZ production cross-section.

4. – Conclusion

A rich programme of Tevatron diboson physics has made huge advances over the ten years of Run 2, testing the standard model, probing for new physics, and underpinning electroweak symmetry-breaking searches. Both experiments have a final dataset of around $10\,\mathrm{fb}^{-1}$, so as well as being combined, these analyses should be updated once more for legacy measurements.

REFERENCES

[1] Campbell J. M. and Ellis R. K., *Phys. Rev. D*, **60** (1999) 113006.
[2] Frixione S. and Webber B. R., *JHEP*, **06** (2002) 029.
[3] Abazov *et al.* (DØ Collaboration), *Phys. Rev. Lett.*, **107** (2011) 241803.
[4] Aaltonen T. *et al.* (CDF Collaboration), arXiv:1202.6629.
[5] Abazov V. M. *et al.* (DØ Collaboration), arXiv:1201.5652v1.
[6] Aaltonen T. *et al.* (CDF Collaboration), *Phys. Rev. Lett.*, **108** (2012) 101801.
[7] Aaltonen T. *et al.* (CDF Collaboration), *Phys. Rev. D*, **85** (2012) 012008.
[8] Aaltonen T. *et al.* (CDF Collaboration), *Phys. Rev. Lett.*, **104** (2010) 101801.
[9] Aaltonen T. *et al.* (CDF Collaboration), *Phys. Rev. Lett.*, **106** (2011) 171801.
[10] Abazov V. M. *et al.* (DØ Collaboration), *Phys. Rev. D*, **80** (2009) 053012.